POWER SYSTEM DYNAMICS MODELING

Máslo K.
ČEPS, a.s. Elektrárenská 774/2, 101 52 Prague, Czech Republic
maslo@ceps.cz

Abstract
Paper deals with power system dynamic modeling, especially from dynamic model verification point of view.

Keywords
Transmission System Operator (TSO), Dispatcher training simulator, Power system dynamic model

1 INTRODUCTION

According to obligations emerged from the European Union energy policy targets (Third Energy Package) ENTSO-E (more information about ENTSO-E is in [1]) adopted a research and development (R&D) plan for common network operation. Four aims are defined in the R&D Plan (according to [2]):

1. to identify the most suitable innovative grid architecture to cope effectively with the 2020 targets,
2. to understand and properly assess the impact and potential benefits of up to date transmission technology,
3. to design and validate novel monitoring and control methodologies of pan- European power system,
4. to develop shared electricity market simulators able to analyze options for market designs and rules.

The R&D Plan contains the basic work streams that are proposed to address the TSO's issues, like advanced and innovative tools e.g. for coordinated operations with stability margin evaluation, for pan-European network reliability assessment, for congestion management.

One of international projects named Umbrella covers these issues. Project has title: Toolbox for Common Forecasting, Risk assessment, and Operational Optimization in Grid Security Cooperations of Transmission System Operators (TSOs) and it is described briefly in chapter 2.

Other work stream of the R&D Plan proposes an improved training tool to ensure better coordination at regional and pan-European level. Such a tool is described in chapter 4.

Dynamic models in some form should be part of both above mentioned tools. Credibility of such dynamic model is a crucial requirement. Chapter 3 deals with this issue.

2 UMBRELA RESEARCH PROJECT

Following paragraphs were adopted from Umbrella description of work.

Transmission system operation is to a large degree influenced by growing share of electricity generation from intermittent renewable energy sources as well as increasing market-based cross border flows and related physical flows. In the mainland central Europe synchronous area due to large installations of renewable energy generation such as wind and photovoltaic, the difference between actual physical flows and the market exchanges can be very substantial. Remedial actions were identified by previous smart grid studies in operational risk assessment, flow control and operational flexibility measures for this area. At the same time an efficient and sustainable power system requires an efficient usage of existing and future transmission capacities to provide a maximum of transportation possibilities. New interconnections and devices for load flow control will be integrated in future transmission networks and will offer new operational options. Further developments of coordinated grid security tools are one of the major challenges TSOs will face in future.

The UMBRELLA research and demonstration project is designed for coping with these challenging issues. The toolbox to be developed will enable TSOs to ensure secure grid operation also in future networks with high penetration of intermittent renewables. The first of the three main objectives of the project is to develop a dedicated innovative toolbox to support the grid security approach of TSOs, which shall include:

a. simulation of uncertainties due to market activities and renewables on different time scales from day-ahead to real time,
b. optimization of corrective actions in reaction to simulated risks on different time scales according to total costs and transmission capacities in the whole system,
c. development of risk based assessment concepts for anticipated system states with and without corrective actions.

Present power system is indubitably very dynamic, so that some dynamic model should be part of the toolbox.

3 DYNAMIC MODEL VERIFICATION

Power system dynamic models (see e.g. [3]) are important part of different tools like network simulator packages, dispatcher training simulators ([4]-[8]) or on-line Dynamic Security Assessment ([9][10][11]). Verification is the most important process in creation of such dynamic models, which are necessary parts of analytical tools. Without validated models is not possible to use any tools for load flow and stability analysis aof power system. Especially if these tools are determined for on-line calculations. This chapter deals with typical examples of such verification process based on comparing of simulation results with measured variables during significant power system disturbance. All simulations were carried out by the MODES network simulator.

3.1 Local disturbance: Double Line to Ground Fault on Double Circuit

This system disturbance occurs on March 23rd 2012 at 17:59:13 of and it affected double line V475 and V476 from the Kočín substation – see single line scheme on following figure:

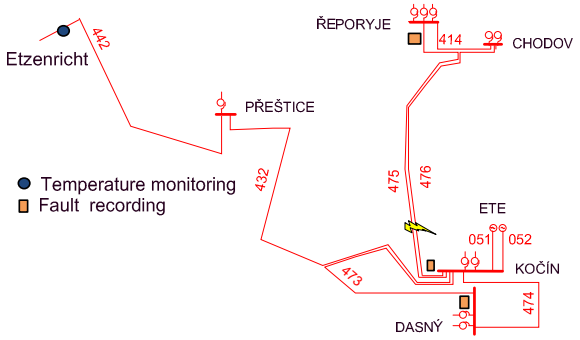

Fig. 1 Single line scheme of affected part of power system

Simultaneous short circuits between phases A, C and ground (caused by strong storm activity) in approximately 32% distance from the Kočín substation were cleared by distance protections in approximately 75 ms.

The same fault was simulated on dynamic model. Initial load flow data (day before snapshot from 22 of March) was used from the DTS, which is described more detailed in chapter 3.2. Model covers in detail power system of the Czech Republic and parts of neighboring systems as is depicted by blue color in Fig. 2.

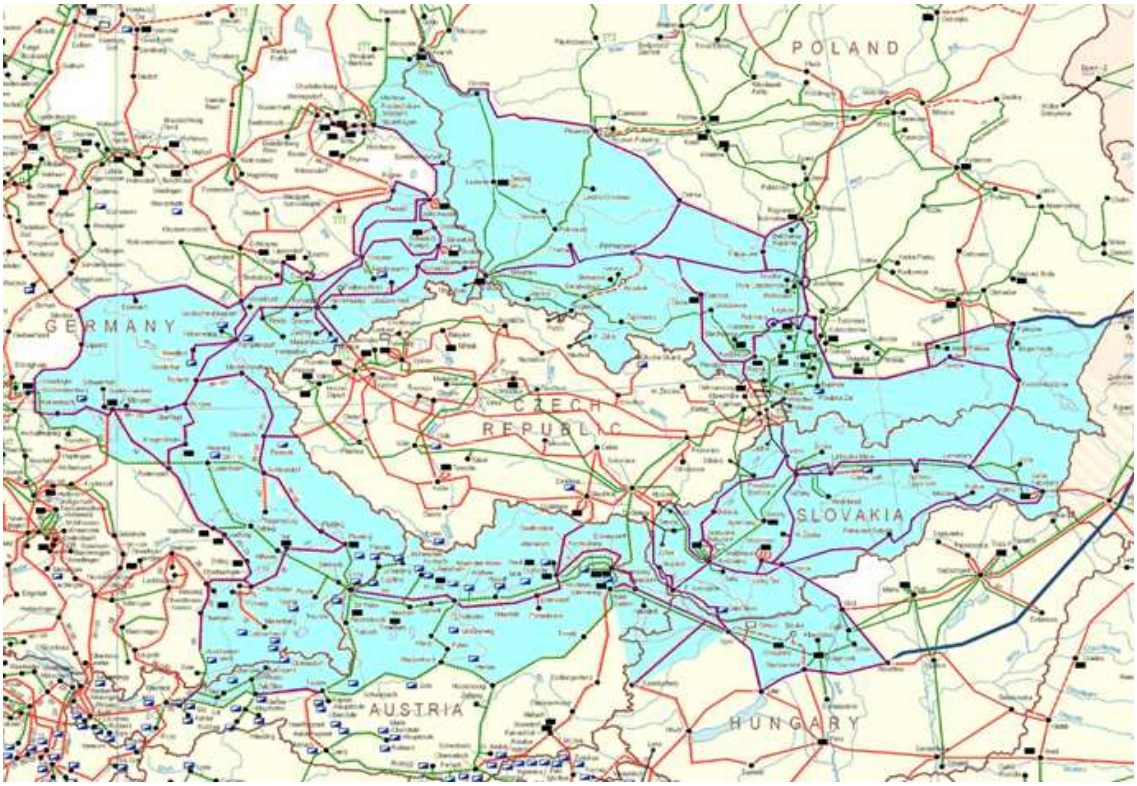

Fig. 2 Single line scheme of observable areas modeled in the DTS

Detailed network model (so called breaker oriented model) represents 5571 nodes, 8 control areas, 9152 branches, 121 three winding transformers (with 50 on load tap changers) and 251 generators. Model contains all necessary equipment like protections (see [12], [13]) and control systems (both load frequency control and automatic V/Q control). Rest of continental Europe was modeled by simple equivalent.

Four sources of measured data were used for verification:

1. Fault recorders (evaluated by SIGRA 4)
2. Power plant monitoring system (NEMES)
3. Energy Management System (EMS)
4. Substation monitoring (TECHSIGHT)

Simulated scenario of events was as follows:

- t=0.1 s: double line to ground short circuit on line V475 (in 32% distance from the Kočín substation, fault rezistance 10 Ω)
- t=0.175 s: fault clearing by distance protection on line V475
- t =0.175 s: switching off of line V476.

Following figures compare records from protection monitoring with simulated time curses for rms values of phase voltages U and currents I in affected phase L1 (with short circuit) and not affected phase L2 (without short circuit).

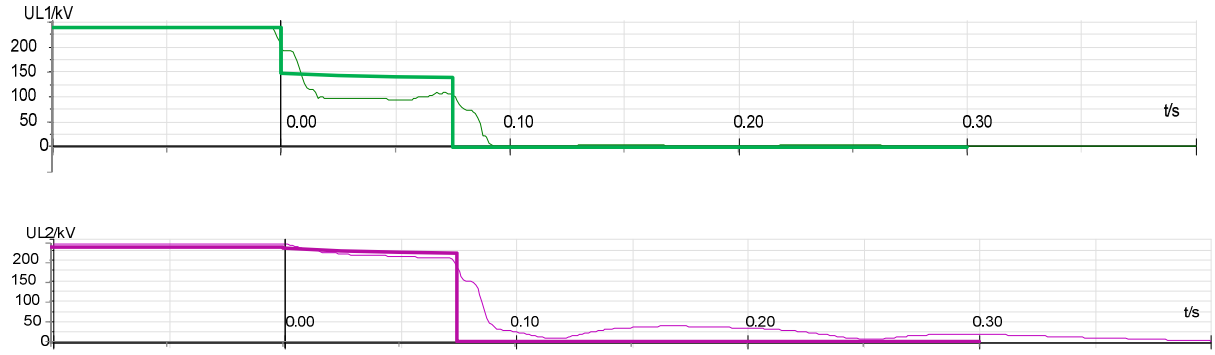

Fig. 3 Measured (thin lines) and simulated (thick) voltages in affected (above) and not affected (below) phases

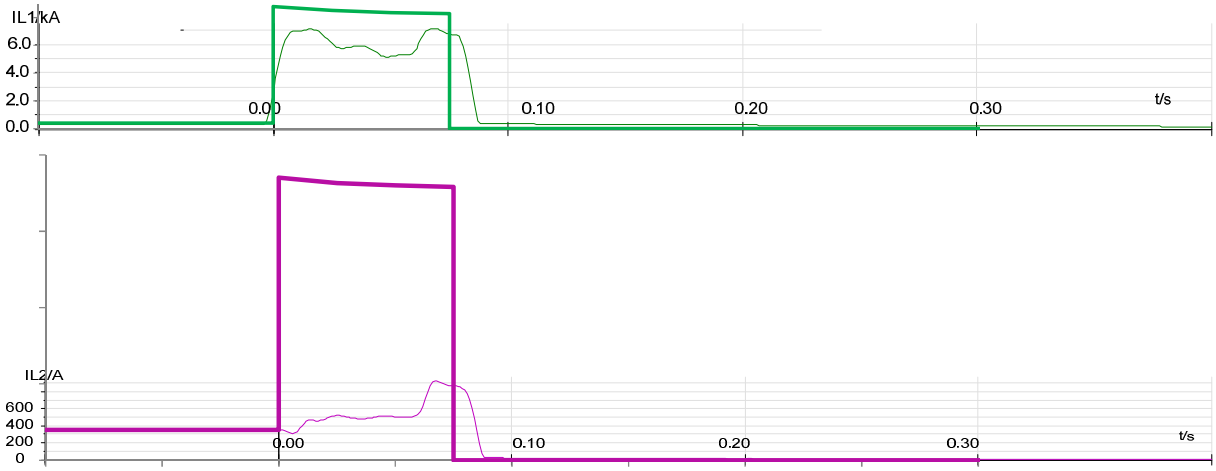

Fig. 4 Measured (thin lines) and simulated (thick) currents in affected (above) and not affected (below) phases

There are significant difference between measuring and simulation for current in not affected phase (Fig. 4 below). Probably reason is way of simulation: short circuit is simulated on the line V475 (and the second line V476 is switched off only), because of only one unsymmetrical fault is possible in one time (simultaneous short circuit is not available in dynamic model).

Fig. 5 shows trajectories of impedances (line do ground) of affected line V475 during fault. Measured time courses from fault recorders (thin lines with marks □ every 1 ms) in the Kočín and Řeporyje substations are compared with results of calculation (thick line with arrows). Measured impedances curl into small balls during short circuits while calculated impedances stay in one place (marked by □ and □) due to neglecting fast electromagnetic transients.

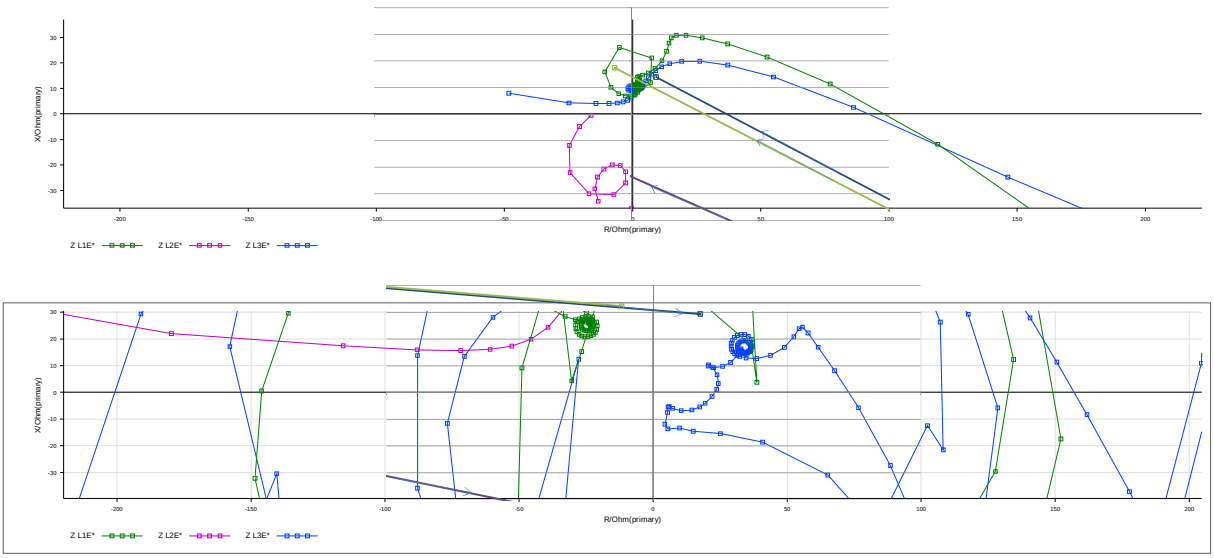

Fig. 5 Measured and simulated line to ground impedances of V475 in the Kočín (above) and Řeporyje subst.

Fig. 6 shows impedance trajectories of near lines (V432 and V473) during fault and after its clearing. Measured time courses from fault recorders (thin lines with marks □ every 1 ms) in the Kočín and Dasný substations are compared with results of calculation (thick line with arrows). Measured impedances curl into small balls during short circuits while calculated impedances stay in one place (marked by □ and □) and then continue to spiral formations during power swings after fault clearing.

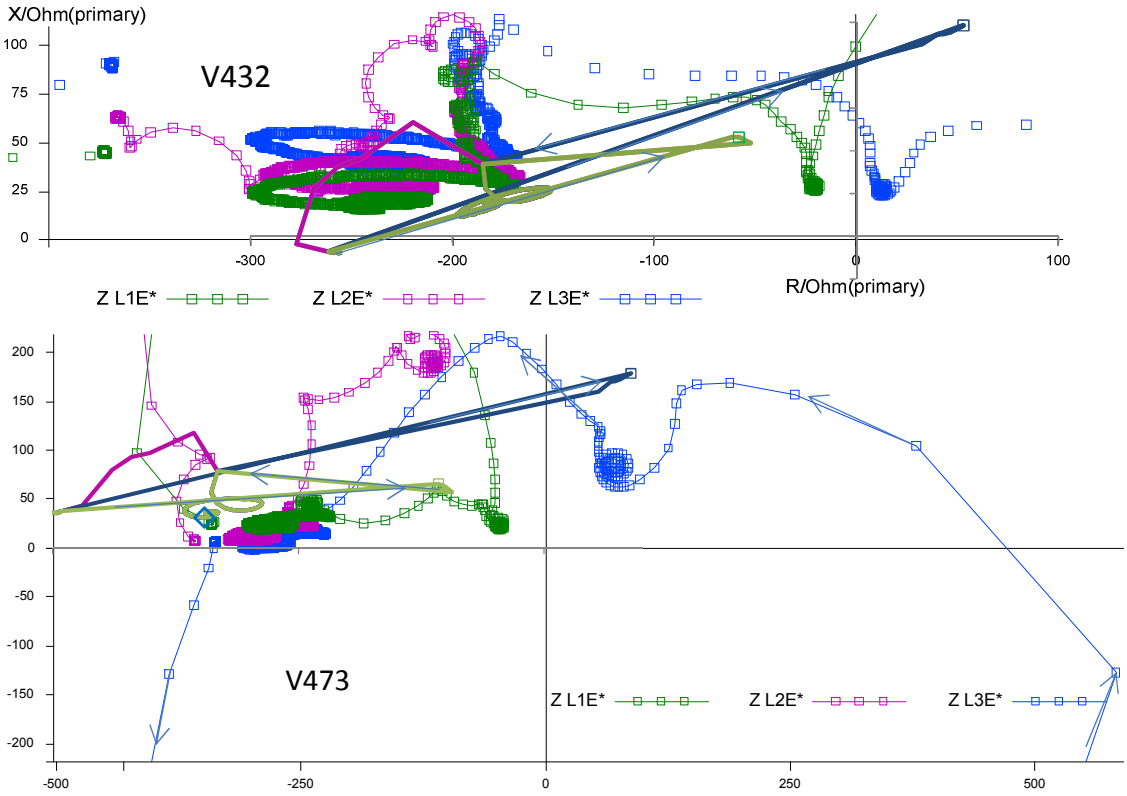

Fig. 6 Measured and simulated impedances of lines V432 in Kočín (above) and V473 in Dasný substations

Trajectory of impedance ZL3E starts in initial state in the first quadrant; it continues according arrow through the fourth and third quadrants (outside of visible area) and wraps to small ball during the short circuit in the second quadrant. Trajectory continues back to the first quadrant and after several swings it finishes in final state near to coordinate origin (final network state is different from initial –two lines are out of operation).

Simulated trajectory is much simpler. It goes from left side of the first quadrant; it continues straight to short circuit point □ in the second. Then trajectory returns to the first quadrant and it finishes after several swings (these swings are in green color for all phases, because network is symmetrical after fault clearing) in final state depicted by ◊ mark.

So series network fault was noticed in near power plant and it triggered power plant monitoring system. Following figure compares measured and simulated active and reactive powers of near unit Temelin (ETE).

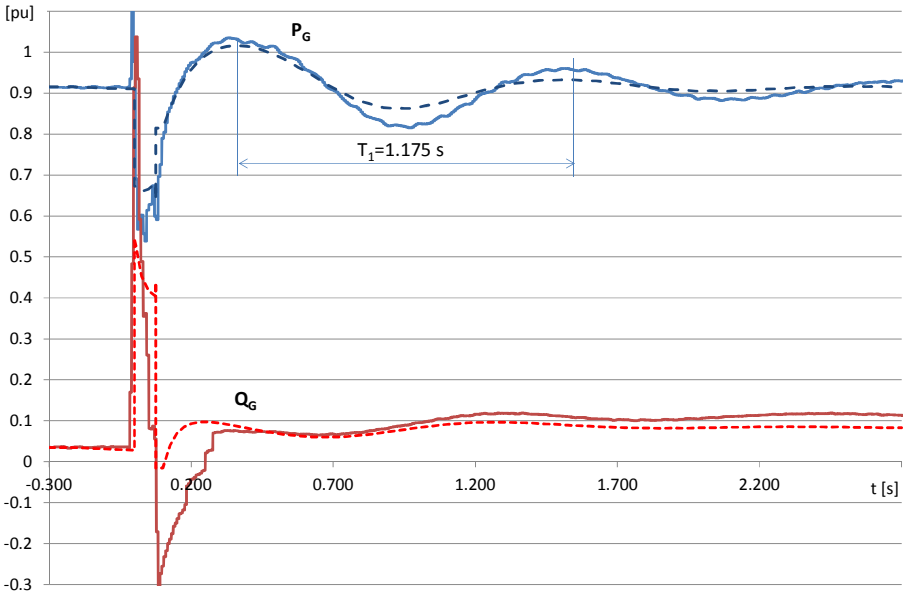

Fig. 7 Measured and simulated (dashed lines) active P_G (blue) and reactive (red) powers of unit ETE

Measured time courses have sampling period 5 ms (so that they include faster electromagnetic transients), while simulated time courses have sampling period 25 ms (so that they include slower electromechanical transients only). Decreasing/increasing of active/reactive powers during short circuit is very similar (except peaks immediately after shot circuit instant – it is caused by neglecting of fast electromagnetic transients in simulation). Swings after short circuit clearing fit perfectly for active power P_G. Swing period T1 are same for real and simulated time courses. It proves that detailed dynamic models of generating unit are used with right parameters. Swing damping is slightly better in simulation. It may be caused by using faster excitation system in model then in real operation (it is seen from reactive power Q_G time courses). It would be analyzed further for improving of dynamic models (as matter of fact creation, validation and improving of dynamic models is never ending process).

So far analyzed time courses belong to so called short term dynamics (till 2.5-5 sec) related to electromechanical phenomena. So called long term dynamics take into account other phenomena like load frequency control (LFC), on load tap changer (OLTC), thermal phenomena in boilers and so on. Similarly conductor temperature comes under this category. Monitoring of conductor temperature is most important part of so called dynamic rating (see e.g. [14]-[17]). Dynamic model of conductor temperature according actual current and weather conditions was implanted in the MODES simulator (describing is in Annex A). Fig. 8 presents real values of current I and temperature T_C of line V442 (tie line between Přeštice and Etzenricht substations) compared with simulated values (dashed lines) during double line outage on 23.3. 2012.

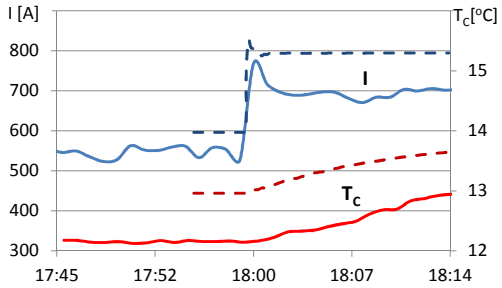

Fig. 8 Comparing of measured and simulated (dashed lines) line current I (blue) and temperature T_C (red)

Increasing of current I caused increasing of conductor temperature. Measuring and simulation show qualitative analogy.

3.2 Global disturbance: partial blackout – power system separation

This system disturbance occurs on January 14th 2012 at 12:42:40 and it affected west part of Turkey (see [18] or [19] for more information about Turkey interconnection with CE power system) – see single line scheme on following figure (affected part is depicted by dashed oval):

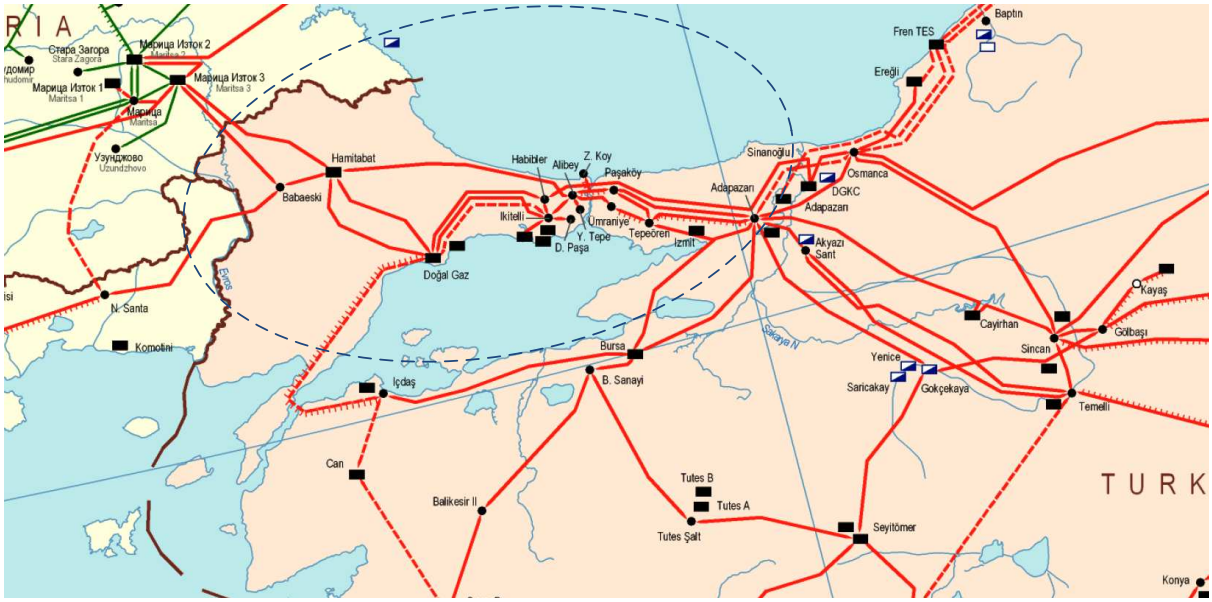

Fig. 9 Single line scheme of partial blackout in Turkey of power system

Accident started by failure of surge arrester at Bursa substation in North-West Turkey due to severe weather conditions (snow and storm). Line -Bursa-Tepepeoren-Adapazari was switched off in the Bursa substation, but switching off in the Adapazari substation was unsuccessful duo to on pole of circuit breaker failure. Circuit breaker failure protection swiched off all lines from one busbar, but duo to telecommunication failure all lines from second busbar of Adapazari substation as well. Continental part stayed connected with the rest of Turkey by only two links to (Adapazari 2 Gaz – Habibler and Adapazari 1 Gaz – Pasakoy). These lines were tripped due to overloading. The remaining lines (double circuit Hamitabat - Maritca 3 and Babaeski - Nea Santa) to the Continental European (CE) system were switched off due to overloading as well and west part of Turkey passed to blackout (other examples of blackout are in [20]). All accident took about four seconds. Father analysis deals only CE power system.

The similar faults were simulated on dynamic model. Initial load flow data was used from the TCS process (TSO Security Cooperation – see [21] - [23] for more information, similar system CORESO is operated in Central Western Europe is described in [24]). These data are based on DACF (Day-Ahead Congestion Forecast) from 14.1.2012 12:30. Model covers all CE system (depicted on Fig. 11). High level of dynamic model elaboration belongs to Central European region, depicted in Fig. 10. The most precise model has of course the Czech Republic. Very detailed model have Hungary, Poland and Slovakia (members of former CENTREL). Relatively detailed model have neighboring systems in Austria and Germany. Rest of CE system has default models for generators, exciters and prime movers.

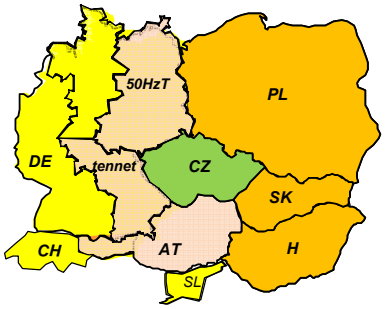

Fig. 10 Block diagram of Central European region

Detailed network model (so called node oriented model) represents 6726 nodes, 27 control areas, 10820 branches and 400 generators. Two sources of measured data were used for verification:

1. WAMS monitoring system (see) provided by swissgrid – (location of WAMS are depicted in Fig. 11)
2. Czech PMU monitoring system.

More information on Wide Area Monitoring System (WAMS) are in [26] - [31].

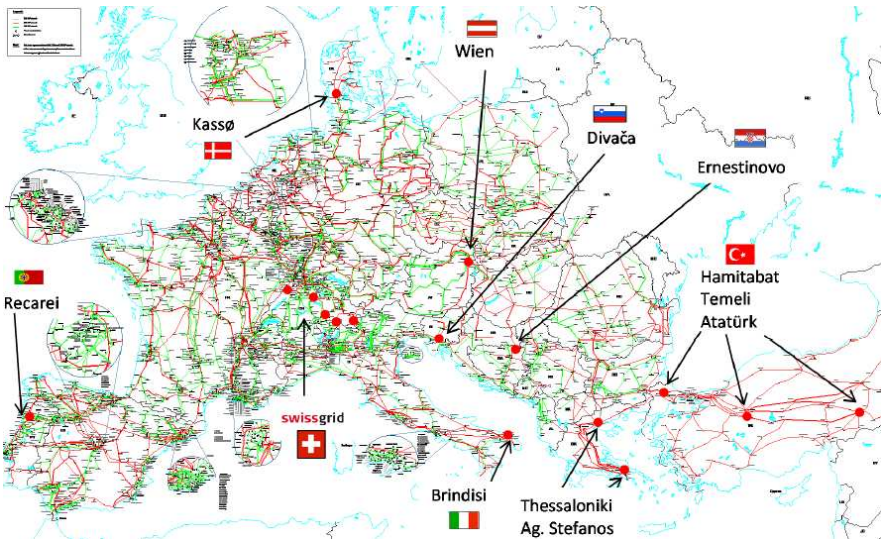

Fig. 11 Current Swissgrid WAMS Links (according [25])

Simulated scenario of events was as follows:

- t=3 s: switching off lines from Adapazari substation
- t=5.5 s switching off lines Adapazari 2 Gaz – Habibler and Adapazari 1 Gaz – Pasakoy
- t =7 s: switching off of line Hamitabat - Maritca 3 and Babaeski - Nea Santa.

Following figures compare time courses from swissgrid monitoring system with simulated time curses for frequencies. Locations of measured frequencies are depicted in Fig. 12.

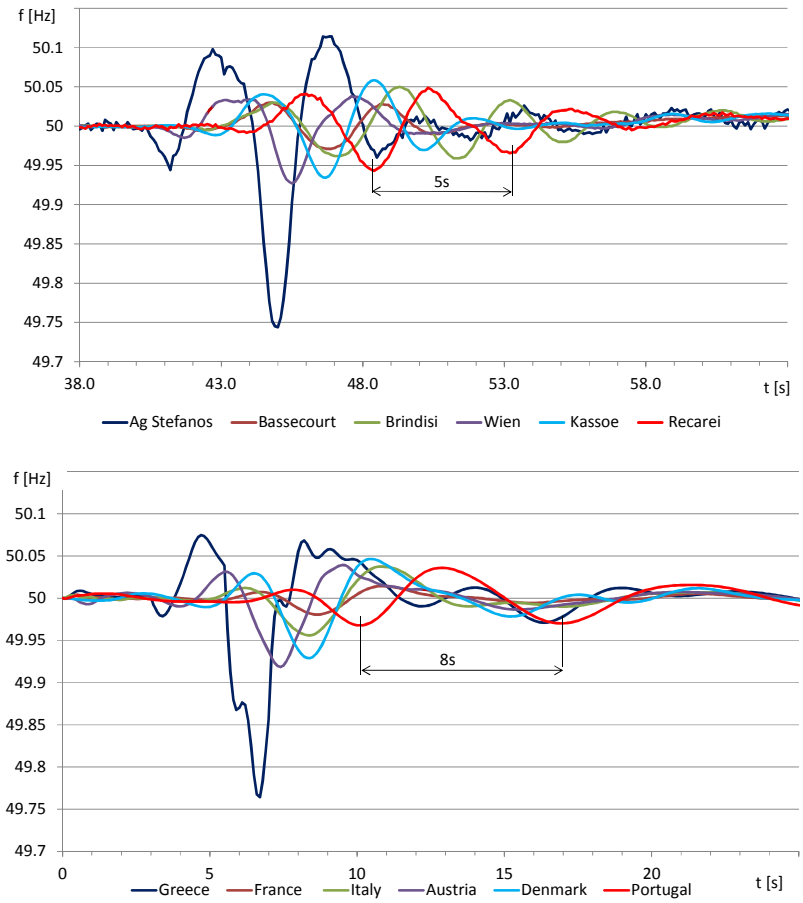

Fig. 13 WAMS measuring (above) and simulated (below) frequencies during Turkey separation

Comparing of measuring with simulation proves credibility of dynamic models. Swing period of interarea oscillations (see [32] and [33]) is somewhat longer, but it cased probably by using of simplified dynamic models in large part of CE (West and Balkan regions). Next fine-tuning of the model may improve accuracy.

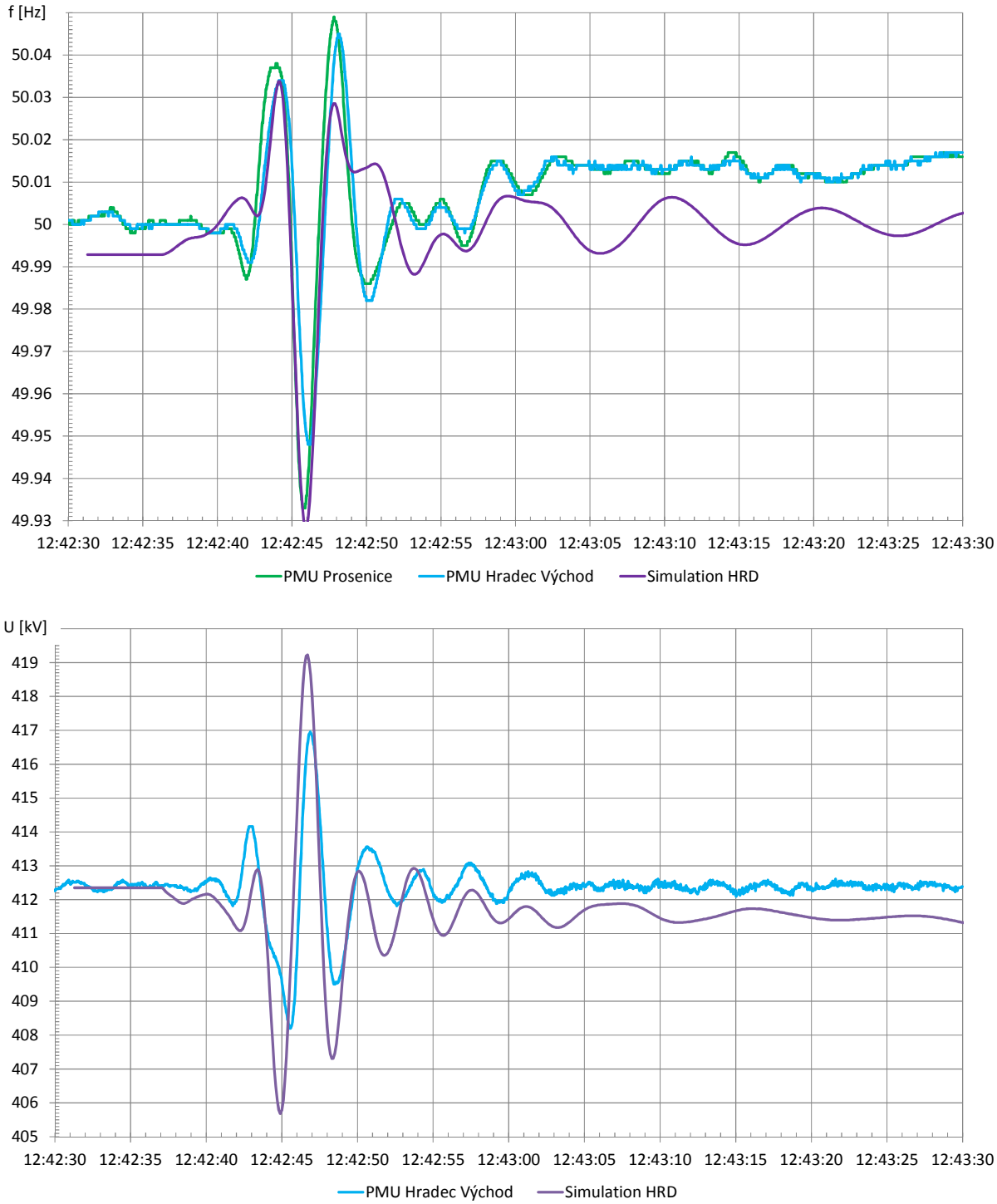

Fig. 14 Comparing PMU measuring and simulated frequencies (above) and voltages (below)

Figures show credibility of used dynamic models.

4 DISPATCHER TRAINING SIMULATOR - DTS

Design specifications (according the R&D Plan [2]) of the future common training center make it possible:

1. to simulate in real time the whole interconnected European power system for training purposes,
2. to train dispatching operators to reproduce and understand large-scale incidents,
3. to provide training on a validated European system model and improve the emergency procedures,
4. to make the DTS available to others such as the power plant or distribution network operators,
5. to develop and test common procedures to face emergency scenarios.

Of course such ambitious specifications are big challenge for authors of power system simulation tools.

4.1 DTS Architecture

Dispatcher training simulators (with some simplification) consist of two main parts: a SCADA (it comprises operational user interface and process data handling) and power system simulation software (so called simulation engine containing necessary models of technical equipment). The simulation engine must be able to communicate with SCADA and vice versa. SCADA sends to simulation engine actual network topology and commands for realistic power system simulation and simulation engine sends back to the SCADA all necessary measured values (voltages, power flows, frequency) and messages about protection and automatics operation.

The above-described arrangement was used in case of a dispatcher training simulator (DTS) implemented in CEPS. Simulation engine from the MODES network simulator (see e.g. [34], [35] or [36]) was transformed into Dynamic Linking Library (called simply DMES) and then integrated into DTS - it is outlined in Fig. 15. The DMES.DLL has three input points called from DTS. Prologue creates proprietary input data files from a data structures sent from DTS. Then the DMES is called periodically from DTS in Simulation. During these simulation steps the DMES saves all commands from DTS into so called journal file. Input and journal files may be used subsequently for off line simulation and analysis in the MODES network simulator environment.

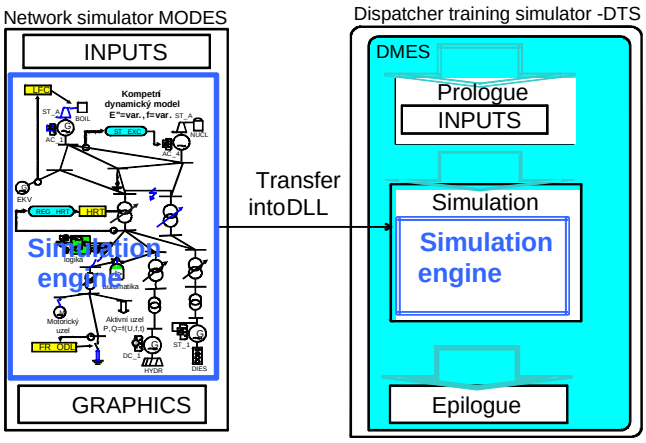

Fig. 15 Integration of power system model into DTS

The DMES is able to comply with the most requirements mentioned in previous chapter, because the same simulation engine was used for many studies. It contains mature and verified models for black start and island operation (see e.g. [37]-[41]), suitable protection models [42] and models of renewable energy sources [43].

4.2 Requirements for DTS

Operational handbook of the former UCTE (but still valid in continental part of ENTSO-E) in Policy 8 [44] defines for simulation engine following functional requirements of DTS:

1. efficient data input, data accessibility and data handling;
2. modeling of all the system components in the operational areas;
3. including low/high voltages, over-current and multi-island-operation;
4. optional modeling of (sub)transient behavior of the system;
5. restoring of the simulated system;
6. combining sets of data of different control areas.

All these common requirements are described in following parts.

Input data for dynamic model (specifically for the DMES) consists of three main parts:

a. static topological data (available in SCADA and corresponding to data for load flow and short circuits calculations)
b. additional data for protections, secondary U/Q control and on load tap changers models (available in Energy management System - EMS)
c. data for dynamic models (they include type of model and parameters for it).

Power system dynamic model should contain all components necessary for realistic power system simulation, namely these particular models for:

1. synchronous and asynchronous generator and excitation system for synchronous generators,
2. prime movers (steam, hydro, gas and wind turbines, internal combustion engine and so on),
3. energy sources (steam boilers, hydro reservoirs and so on),
4. energy conversion systems like photovoltaic power plants (called Power Park Modules as well),
5. load (lighting and heating, induction motors, static characteristic and so on),)
6. secondary U/Q and f/P (called load frequency control as well) controls
7. on load tap changers for normal transformers and for phase shifting transformers,
8. network protection (distance, overcurrent and so on) and special protection schemes,
9. FACTS and HVDC.

If all above mentioned models are suitable implemented, it is possible to simulate different not only ordinary system states during normal power system operation, but disturbed system states with not nominal voltage, currents and frequencies and moreover power system restoration process as well.

Combining sets of data of different control areas is necessary for inter TSO dispatcher training and for improving of power system model accuracy as well.

5 CONCLUSIONS

Dynamic models create essential part of different tools for power system analysis and simulation. They creation and improvement is long term process and they requires permanent verification, preferably by comparing of measured and calculated time courses. Paper presents such verification for two typical power system disturbances.

The first case is local power system dynamic behavior after short circuits represented by local electromechanical oscillations (with frequencies 1-2 Hz). Fault recorders from substations and power plants are useful aids for accuracy of power system models evaluation.

The second case global power system dynamic behavior after part of system separation represented by global inter-area oscillations (with frequencies 0.1 - 1 Hz). WAMS is excellent source of information for verification of dynamic models.

Investigation of power system dynamic behavior during such disturbances is important part power system stability analysis – it is rotor angle stability according classical classification from [45]. The first case represents so called transient stability and second one represents so called small-disturbance angle stability.

6 ACKNOWLEDGEMENTS

This paper is partially supported from research project Umbrella which is funded under the 7th Framework programme of the EU - theme ENERGY.2011.7.2-1: Innovative tools for the future coordinated and stable operation of the pan-European electricity transmission system.

The author acknowledges the information about Turkey blackout provided by W. Sattinger from Swissgrid (Transmission System Operator in Switzerland).

7 REFERENCES

[1] Máslo K.: Challenges to power system operation and development, the 6th International Scientific Symposium on Electrical Power Engineering 2011, St. Lesná, Slovakia, ISBN 978-80-553-0724-4

[2] ENTSO-E R&D Plan -European grid towards 2020 challenges, available online at https://www.entsoe.eu/fileadmin/user_upload/_library/Key_Documents/100331_ENTSOE_R_D_Plan_FINAL.pdf

[3] Ruhle O, Balasin F.:Simulations of Power System Dynamic Phenomena, 2009 IEEE PowerTech Conference, Bucharest

[4] Stubbe M. at al.: Training operators to acute system contingencies, CIGRE Session 2006, Paris

[5] Bruno S. at al.: Emergency control assessment for mitigating the effects of cascading outages, CIGRE Session 2006, Paris

[6] Carrano A. at al.: The new DTS for the Italian transmission system dispatcher: organisation, architecture, tools and functionalities, CIGRE Session 2008, Paris

[7] Istardi D. at al.:Understanding Power System Voltage Collapses using ARISTO: Effects of Protection, 2009 IEEE PowerTech Conference, Bucharest

[8] Rabinovich M.A., Morjin J.I., Potapenko S.P.: Digital Model Power Systems of Real Time for Information Support of Dispatcher Power Systems, CIGRE Session 2010, Paris

[9] Massucco S.: Advanced perspectives and implementation of Dynamic security Assessment in the open market environment, CIGRE Session 2002, Paris

[10] Krebs R. at al.; Blackout prevention by online network and protection security assessment: 1st DSA-experiences from North Africa, CIGRE Session 2008, Paris

[11] Giannmuzzi G. at al.: On-Line Analysis of the Electrical System Security: an Extensive Simulation Approach in a Dynamic Security Assessment (DSA) Environment, CIGRE Session 2010, Paris

[12] Bozek M.: Distance protection algorithm for double-circuit transmission line with fault resistance compensation, 17th Power Systems Computation Conference , Stockholm 2011

[13] Máslo K., Kaňok M.: Distance Protection Model for Network Simulators, the 8th International Conference CONTROL OF POWER SYSTEMS 2008, Štrbské Pleso, ISBN 978-80-2227-2883-6

[14] Douglas D.A., Edris A., Pritchard G. A.: Field Application of a Dynamic Thermal Circuit Rating Method, IEEE Transactions on Power Delivery, Vol. 12, No. 2, 1997

[15] Ringelband T., Lange M., Dietrich M, Haubrich H.: Potential of Improved Wind Integration by Dynamic Thermal Rating of Overhead Lines, IEEE Bucharest Power Tech Conference 2009, Bucharest

[16] Cloet E., Lilien J-L., Ferrieres P.: Experiences of the Belgian and French TSOs using the "Ampacimon" real-time dynamic rating system, CIGRE Session 2010, Paris

[17] Kazerooni A. K. at al.: Dynamic thermal rating application to facilitate wind energy integration, IEEE PowerTech 2011, Trondheim

[18] Ilicito F. :Special protection system in the interface between the Turkish and ENTSO-E power systems to counteract propagation of major disturbances, CIGRE Session 2010, Paris

[19] Al-Ali S., Nassar I., Weber H.: Interconnection of the European ENTSO-E-CE system with the Turkish system: Investigation of the inter-area oscillations behaviour, 17th Power Systems Computation Conference, Stockholm 2011

[20] Meng D. Z.: Maintaining System Integrity to Prevent Cascading Blackout, CIGRE Session 2006, Paris

[21] Kranhold M. at al.: Increased cooperation between TSO as a precondition for coping with new challenges in system operation, CIGRE Session 2010, Paris

[22] Klaar D.: New TSO coordination initiative in Europe, CIGRE Session 2010, Paris

[23] Máslo K., Galetka M.: Security operation of transmission network - present time and future challenges, 12th International Conference Electric Power Engineering 2011, Dlouhé Stráně, ISBN 978-80-248-2393-5

[24] Boulet F.: Lessons learnt after one year of running a technical coordination service centre in the Central Western Europe, CIGRE Session 2010, Paris

[25] W. Sattinger: Application of PMU measurements in Europe TSO approach and experience , IEEE Trondheim PowerTech 2011

[26] Cirio D. at al.: Wide Area Monitoring and Control System: the Italian research and development

[27] Sattinger W., Bertsch J., Reinhard P.: Operational experience with WAMS, CIGRE Session 2006, Paris

[28] W. Sattinger: Awareness system based on synchronized phasor measurements, IEEE Power & Energy Society General Meeting 2009.

[29] G. Giannuzzi at al.: Voltage and angle stability monitoring: possible approaches in the framework of WAMS, CIGRE Session 2008, Paris

[30] Wilson D. H.: Control Centre Applications of Integrated WAMS-based Dynamics Monitoring and Energy Management Systems, CIGRE Session 2008, Paris

[31] Moxley R., Zweigle G.: Real-time, wide-area measurements for improved operator response, CIGRE Session 2010, Paris

[32] Grebe E.: Analysis and Damping of Inter-Area Oscillations in the UCTE/CENTREL Power System, CIGRE Session 2000, Paris

[33] E. Grebe at al.: Low frequency oscillations in the interconnected system of Continental Europe , Power and Energy Society General Meeting, 2010 IEEE

[34] Máslo K.: The general purpose network simulator MODES, the 4th international workshop on EPSCC 1997, Rethymno, Greece

[35] Máslo K., Neuman P.: Power System and Power Plant Dynamic Simulation, the 15th IFAC World Congress 1999, Beijing, China, ISBN 0-08-043248-4, Volume O, pg. 179-184

[36] Máslo K., Feist J.: Power system dynamics behavior, modeling and simulation, the 2nd international workshop on EPSCC 1993, Alghero, Italy

[37] Máslo K., Vnoucek S., Fantík J.: Unit black start and power system restoration , the international symposium MEPS 1996, Wroclaw, Poland

[38] Máslo K., Fantík J.: Dynamic analysis of the Power System, the 2nd international conference CPS 1996, Bratislava, Slovakia.

[39] Máslo K., Petruzela I., Piroutek Z.: Nuclear power plant in island operation, the 32nd conference UPEC 1997, Manchester, England

[40] Máslo K., Anděl J.: Gas turbine model using in design of heat and power stations, IEEE PowerTech conference 2001, Porto, Portugal, ISBN 0-7803-7140-2

[41] Borghetti A., Paolone M., Maslo K., Petružela I., Spelta S.: Steam unit and gas turbine power station reliable control for network black-start-up, IEEE PowerTech 2003, Bologna, Italy , ISBN 0-7803-7968-3

[42] Máslo K.: Distance protection model for network simulators, the 14th IEEE MELECON conference 2008, Ajaccio, France, ISBN 978-1-4244-1633-2

[43] Máslo K., Pistora M.: Long term dynamics modeling of renewable energy sources, IEEE EUROCON international conference on computer as a tool 2011, Lisbon, Portugal, ISBN 978-1-4244-7485-1

[44] UCTE OH – Policy 8: Operational Training (final version 1.0, 13.03.2008) , available online at https://www.entsoe.eu/fileadmin/user_upload/_library/publications/entsoe/Operation_Handbook/Policy_8_final.pdf

[45] Definition and classification of power system stability, CIGRE technical brochure No. 321. Paris 2003

[46] IEEE Std. 738-2006 for calculating the current temperature of bare overhead conductors

8 ANNEX A: EQUATIONS FOR CONDUCTOR TEMPERATURE EVUALATION

Equations for computer calculation of conductor temperature implemented in the MODES network simulator are described in this chapter.

8.1 Non-steady heat balance

Differential equation for mean conductor temperature T_C (average of core and surface temperature) describes heat power balance as follows:

$$Mc_P \frac{dT_C}{dt} = RI^2 + P_S - P_R - P_C \quad [W/m] \tag{1}$$

Mc_P [J/m °C^{-1}]. conductor heat capacity (mass per unit length M x specific heat of conductor c_P)

R [Ω/m] ..... conductor resistance (it may be dependent on T_C: $R = R_{20}[1+0.004(T_C-20)]$)

I [A] ..... current

P_S [W/m]..... heat gain rate from sun per length

P_R , P_C [W/m] . radiated and convected heat loss rate per length

While conductor resistance and current are known in network simulator, other variables should be calculated specially.

8.2 Rate of solar heat gain

Rate of solar heat can be calculated according equation:

$$P_S = \alpha D P_{SE} \sin\theta / 1000 \quad [W/m] \tag{2}$$

α [-] .....solar absorptivity (0-23 -0.91)

D [mm]..... conductor diameter

P_{SE} [W/m^2].....total solar radiated heat flux rate

θ [°] .....angle of incidence of the sun's rays

Angle between sun's rays and conductor axis:

$$\theta = \arccos\{\cos H_C \cdot \cos(Z_C - Z_L)\} \ [^\circ] \tag{3}$$

H_C, Z_C [°].....altitude and azimuth of sun

Z_L [°] .....azimuth of line

Altitude and azimuth of sun is calculated as follows:

$$H_C = \arcsin\{\sin L_{at} \cdot \sin\delta - \cos L_{at} \cdot \cos\delta \cdot \cos(15T)\} \ [^\circ]$$

$$\delta = 23.45 \sin\left\{\frac{284+N}{365}360\right\} \quad [^\circ] \tag{4}$$

$Z_C=\beta$ for T≤12 or $Z_C=360-\beta$ for T>12 $\quad \beta = \arccos\left\{\dfrac{\cos L_{at} \sin\delta + \sin L_{at} \cos\delta \cdot \cos(15T)}{\cos H_C}\right\}$ [°]

L_{at} [°] .....degrees of geographical latitude (approximately 50 °for Czech Republic)

T [hour] .....sun time (it is equal approximately to central CET for Czech Republic)

δ [°] .....solar declination (0-90)

N [-] .....numerical order of day of the year (1-365)

According [46] is possible to calculate total solar radiated flux rate with help of approximation:

$$P_{SE} = (A + BH_C + CH_C^2 + DH_C^3 + EH_C^4 + FH_C^5 + GH_C^6)(I + JH_E + KH_E^2) \quad [W/m^2] \tag{5}$$

A,B,C,D,E,F,G,I,J,K parameters of approximation

H_E [m] ..... elevation of conductor above sea level

But it is possible to use more simple approximation:

$$P_{SE} = P_0 \cdot e^{-0{,}1z\left(\frac{16000-H_E}{16000+H_E}\cdot\frac{1}{\sin H_C}\right)^{0{,}8}} \quad [W/m^2] \qquad (6)$$

P_0 [W/m^2].....sun constant (approximately 1370 W/m^2)

z [W/m^2] .....Linke turbidity coefficient (2-4 for clear atmosphere and sky)

Values of P_{SE} according equations (5) and (6) are depicted in the following figure by full and dotted red line. Shapes of the curves are practically same.

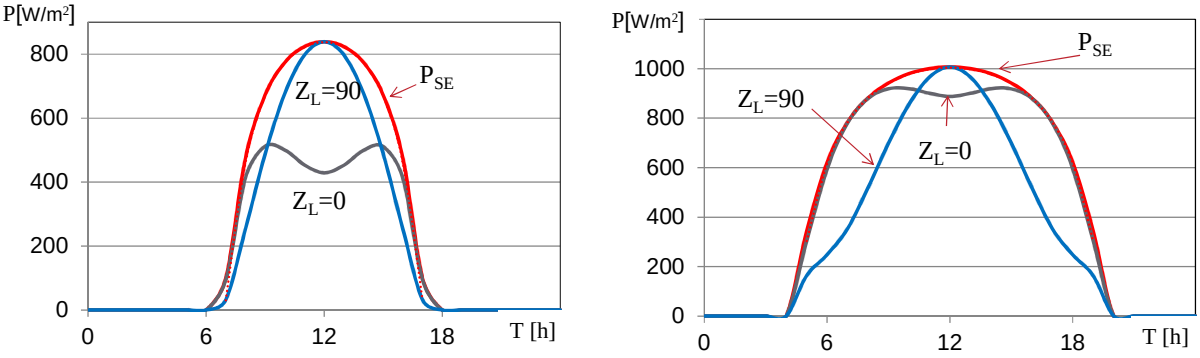

Fig. 1 Solar radiated heat flux rates for winter day N=15 (on the left) and summer day N=195 (on the right)

Total solar radiated heat flux rate for two orientation lines (with azimuth Z_L=0^o and Z_L=90^o) are depicted as well.

8.3 Rate of radiated heat loss

Rate of radiated heat loss P_R can be calculated according equation:

$$P_R = 0.0178 * 10^{-8}\,\varepsilon \cdot D \cdot \left[(T_C + 273)^4 - (T_a + 273)^4\right] \quad [W/m] \qquad (7)$$

ε [-] .....heat emissivity (0-23 -0.91)

T_a [^{o}C] .....ambient air temperature

8.4 Rate of convection heat loss

According [46] there three equations for convection heat loss evaluation for low wind speed P_{C1}, high wind speed P_{C2} and natural convection P_{Cn}:

$$P_{C1} = \left[1.01 + 0.0372(D * v_W/\nu)^{0.52}\right] k_f\, k_W\, (T_C - T_a) \quad [W/m]$$

$$P_{C2} = \left[0.0119(D * v_W/\nu)^{0.6}\right] k_f\, k_W\, (T_C - T_a) \quad [W/m] \qquad (8)$$

$$P_{Cn} = .0205\rho_f{}^{0.5} D^{0.75} (T_C - T_a)^{1.25} \quad [W/m]$$

v_W [m/s]..... wind speed

ν [m^2/s] ..... kinematic viscosity of air $\nu = 10^{-7}(133 + 0.96\,T_f + 0.019\,H_E + 0.000113\,H_E T_f)$

ρ_f [kg/m^3]..... density of air $\rho_f = (1.293 - 0.0001525\,H_E + 0.000000006379 H_E{}^2)/(1 + 0.00367 T_f)$

k_f [W·m^{-1}·^{o}C^{-1}] thermal conductivity of air $k_f = 0.0242 + 0.00007477 T_f + (0.0000638 T_f)^2$

k_W [-] ..... wind direction factor for angle Φ $k_w = 1.194 - \cos\Phi + 0.194\cos 2\Phi + 0.364\sin 2\Phi$

T_f [^{o}C].....$T_f = (T_C + T_a)/2$

IEEE standard [46] recommends to use the highest value from P_{C1}, P_{C2} and P_{Cn} for a given wind conditions. These values are depicted on Fig. 2. Approximately till v_W-1.7 m/s is $P_{C1} > P_{C2}$.. Allowed conductor current I is calculated from the steady - state balance for conductor rezistance R=0.0000624:

$$I = \sqrt{\frac{P_R + P_C - P_S}{R}}\ [A] \qquad (9)$$

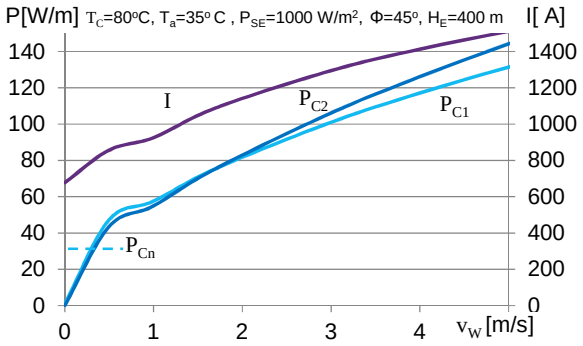

Fig. 2 Dependency of particular convection heat losses P_C on winds speed v_W for conductor 450Fe8

8.5 Wind speed

Wind speed time course can be evaluated by approximation already published in [43]:

$$v_W = v_{mean}\left[Ae^{-\left(\frac{T-\mu}{\sqrt{2}\sigma}\right)^2} + A_0 \right] \quad [m/s] \tag{10}$$

Examples of used parameters are in the following table:

Tab. 1 List of parameters for wind speed approximation

Month	A	μ	σ	A_0	v_{mean}
January	0.17	11.963	2.531	0.955	2
July	0.71	12.49	4.14	0.69	1

8.6 Ambient temperature

Ambient temperature time course can be evaluated by approximation:

$$T_a = Ae^{-\left(\frac{T-\mu}{\sqrt{2}\sigma}\right)^2} + A_1 \sin(\omega_1 T + \varphi_1) + A_2 \sin(\omega_2 T + \varphi_2) + A_0 \quad [^oC] \tag{11}$$

Examples of used parameters are in the following table:

Tab. 2 List of parameters for ambient temperature approximation

Month	A	μ	σ	A_1	ω_1	φ_1	A_0	A_2	ω_2	φ_2
January	2.14	13.53	2.84	-0.43	0.27	5.14	-1.30	-0.14	31.64	0.91
July	21.53	14.84	6.68	-8.90	6.42	12.22	9.89	-0.56	9078.47	55.74

Comparing on Fig. 3 shows negligible difference between long temperature normal (for Czech Republic) and approximation.

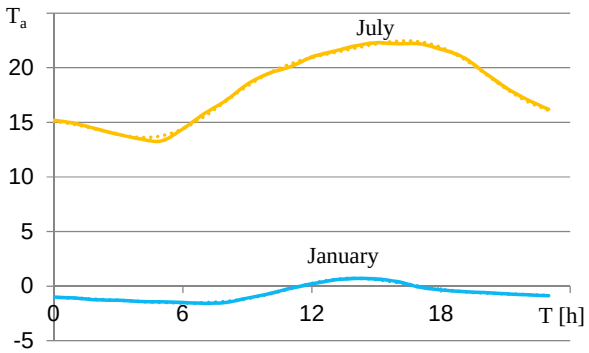

Fig. 3 Comparing normal of long term ambient temperature (full line) with approximation (dotted line)

8.7 Conductor temperature dynamic model¨

Basic structure of the model is suggested in the following figure.

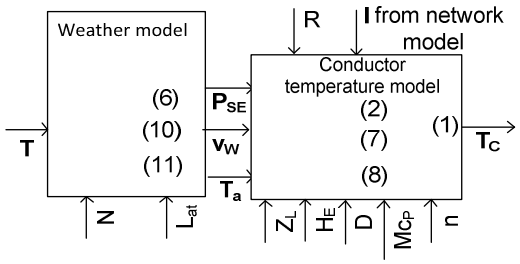

Fig. 4 Simplified structure of conductor temperature model

There are two input variables day time T (it is derived from current simulation tome t) and line current (output from the network model, for bundled conductors should be divide by number of conductors in the bundle – usually 3 for 400 kV lines). In weather model three weather variables P_{SE}, v_W and T_a are calculated from equations (6) ,(10) and (11). Necessary parameters are collected in following table:

Tab. 3 List of typical parameters for weather model for Czech Republic

	Sunshine				Wind speed					Ambient temperature									
Param.	N	L_{at}	P_0	z	A	μ	σ	A_0	v_{mean}	A	μ	σ	A_1	ω_1	φ_1	A_0	A_2	ω_2	φ_2
January	15	50	1400	3	0.17	11.963	2.531	0.955	2	2.14	13.53	2.84	-0.43	0.27	5.14	-1.3	-0.14	31.64	0.91
July	195	50	1400	3	0.71	12.49	4.14	0.69	1	21.53	14.84	6.68	-8.9	6.42	12.22	9.9	-0.56	9078	55.74

Calculated weather variables are considered same for whole control area for the first approximation (of course this model could be refined in future by using GPS location and more detailed weather model). Particular heat losses and gains are calculated from weather variables and conductor current by equations (2), (7) and (8). Heat power balance differential equation (1) is resolved finally. Necessary parameters are collected in following table:

Tab. 4 List of parameters for conductor temperature model for typical 400 kV ropes

Param.	n	Mc_{pt} [$Jm^{-1}K^{-1}$]	Z_l [°]	H_E [m]	D[mm]	R [Ω/m]	ε=α
450Fe8	3	1300	90	400	28.7	0.0000674	0.5
350Fe6	3	1066	90	400	22.8	0.00008	0.5